ELSEVIER

PII: S0032-3861(98)00020-2

Polymer Vol. 39 No. 25, pp. 6441–6447, 1998

0032-3861/98/$ - see front matter

Effect of EGMA content on the tensile and impact properties of poly(phenylene sulfide) EGMA blends

Sang Il Lee and Byoung Chul Chun*
Department of Polymer Engineering, College of Engineering, The University of Suwon, San 2-2, Wawu-ri, Bongdam-myon, Hwasung-gun, Kyonggi-do, Korea
(Received 2 September 1997; revised 18 November 1997; accepted 5 December 1997)

Mechanical properties of poly(phenylene sulfide)(PPS)/poly(ethylene-stat-glycidyl methacrylate)-graft-poly-(acrylonitrile-stat-styrene)(EGMA) blends at various testing temperatures (−50°C, 25°C and 150°C) and EGMA contents (0, 2, 5, 10 and 20 wt.%) were investigated. Also the tensile and impact fractured surface and inner subsurface microstructures were investigated using scanning electron microscopy (SEM) and polarized optical microscopy (POM). Maximum stress and notched Izod impact test results showed that 5 wt.% EGMA inclusion exhibited higher mechanical properties than any other compositions except 20 wt.% EGMA inclusion at a 150°C testing condition. POM observation of tensile tested subsurface microstructure showed that the plastic deformation bands were formed 90° to the tensile direction in 80 wt.%PPS/20 wt.%EGMA blend. Average EGMA particle size increased with EGMA content, however, EGMA particle size distribution decreased up to 5 wt.% EGMA inclusion, then started to increase above this composition. SEM observation of tensile fractured 95 wt.%PPS/5 wt.%EGMA blend tested at 150°C showed a more plastic deformation than any other blend compositions. From these results, it is concluded that 95 wt.%PPS/5 wt.%EGMA blend had the highest tensile and impact strength.

(Keywords: poly(phenylene sulfide); tensile property; impact property)

INTRODUCTION

PPS was first commercialized by Philips Petroleum Co. in 1973 as a trade name of Ryton, and since then its application has expanded into electrical, electronic, automotive and precision molded articles due to its superior heat resistance, dimensional stability and insulating properties[1]. PPS is synthesized from sodium sulfide (Na_2S) and *p*-dichlorobenzene (PDCB) in an organic solvent and has simple repeating units. Due to this chemical structure, PPS is sometimes called poly(arylene sulfide) (PAS) or poly(*p*-phenylene sulfide). PPS can be recycled without much deterioration of properties, thus this can reduce the environmental problems[2].

PPS has a glass transition temperature of 85°C–90°C and melting temperature of about 290°C, and does not dissolve in any solvent below 200°C except strong acid. Even though PPS has these advantageous properties, it has weaknesses such as low impact strength and presents difficulties in injection molding. In order to overcome these problems, there have been studies on the crystallization and melting behaviour of PPS and its composites in recent years[2–8]. Also the studies on the various PPS blends were performed[9–15]. Advantages of blending are well known because it can reduce the price of expensive component by blending with an inexpensive component, and it can also improve the properties of one component from the additive rule, and especially in the case of incompatible blends, these properties are dependent on the dispersed particle size and volume fraction[14].

Generally, in order to improve the impact and toughness of brittle polymers, it is common practice to add ductile polymers to the matrix. Research on the fracture behaviour of polymer blends are generally concerned with the dispersed particles in the matrix which can hold the crack propagation or promote shear yielding to improve the mechanical properties. At present time, there are several published studies on PPS blends and composites, however, these are mainly concerned with the thermal and crystallization behaviour, and not many studies are available on the structure–property relationships of these blends. Thus, in this investigation, PPS was blended with EGMA in order to improve the tensile and impact properties, and its fracture morphologies were investigated at different testing temperatures (−50°C, 25°C and 150°C) and the resultant structure–property relationships were studied.

EXPERIMENTAL

Materials and sample preparation

PPS used in this investigation was a commercial grade resin (SKI, Suntra S-500, $M_W = 30\,000$ g mol^{-1}). Impact modifier EGMA was also a commercial grade obtained from the Nippon Oil and Fats Co. (Grade A4400, M.I. = 0.3 g/10 min, density = 0.97 g cm^{-3}). *Table 1* shows the compositions and sample code of PPS/EGMA blends prepared in this investigation. Compounding was done using twin screw extruder (Toshiba, co-rotating intermeshing type, $\phi =$ 35 mm), and the screw rpm was 350 and the temperature was maintained at 315°C–320°C. Tensile and impact specimens were manufactured according to ASTM specifications using an injection molder (Engel ES 240/75P).

* To whom correspondence should be addressed. Tel:0331 220 2476; Fax: 0331 220 2494

Table 1 Compositions and sample code of PPS/EGMA blends used in this investigation

PPS/EGMA (wt.%)	100/0	98/2	95/5	90/10	80/20	0/100
Sample code	PPS 1	PPS2	PPS3	PPS4	PPS5	EGMA

Mechanical property measurement

Lloyd instrument (LR 50K) was used for the tensile test, and gauge length was 100 mm and crosshead speed was 50 mm min^{-1}. Testing temperature was −50°C, 25°C and 150°C, respectively, and storage time was changed from 1, 2, 6 and 24 h, and storage time variation did not affect the tensile properties after 1 h, thus all specimens were preconditioned for 1 h. At least five specimens were tested and the average value was used for the data plot. Notched Izod impact strength was measured using the Testing Machines Inc. (model 43-02, Pendulum 75 kgcm, Izod type). All specimens were manufactured to the ASTM D-256 specification (thickness: 6.35 mm), and storage time was set to 1 h as in tensile testing. At least 10 specimens were tested at −50°C, 25°C and 150°C, and the average value was used for the data plot except the maximum and minimum values.

Density measurement

Densities were measured using the density gradient column (Lloyd Instrument, Davenport 2-column densitometer). Acetone (JIN Chemical, density = 0.798 g cm^{-3}) and carbon tetrachloride (Ducksan Chemical, density = 1.608 g cm^{-3}) was used as a gradient solution, and at least 10 standard floats were used to ensure good calibration line. Temperature of the column was maintained at 23 ± 0.1°C. At least three samples were floated in the column and average height was used for density calculation.

Morphology analysis

POM (Nikon, Optiphot 2-POL) was used for observing EGMA particle size and distributions in the PPS matrix. In order to observe this distribution, specimens were prepared using a grinding–polishing machine (Buehler UK Ltd. Metaserv 2000). From these polished specimens, particle size and distribution were examined from the POM connected directly to the image analyser (Image Pro plus for window 1.2) and the obtained image was analysed directly. Impact and tensile fractured surfaces were also examined using scanning electron microscope (JEOL, model JSM-5200). Operating voltage was 25 kV.

RESULTS AND DISCUSSION

EGMA particle size, distribution and size distribution

Figure 1 shows the EGMA particle size and distribution with 95% confidence limit and *Figure 2* shows the POM photographs of PPS3 and PPS5. POM observation shows that the average EGMA particle size and size distribution increases as the EGMA content increases, and especially at more than 5 wt.% EGMA inclusion, the distribution increases more rapidly. Especially, EGMA particle size distribution decreased up to PPS3 which has the narrowest particle size distribution, and increased thereafter. This particle size increase is due to the coalescence of EGMA particles during the melt mixing process, and this size change is also affected by the interfacial interaction, melt viscosity, melt elasticity and other processing parameters of constituent polymers[15].

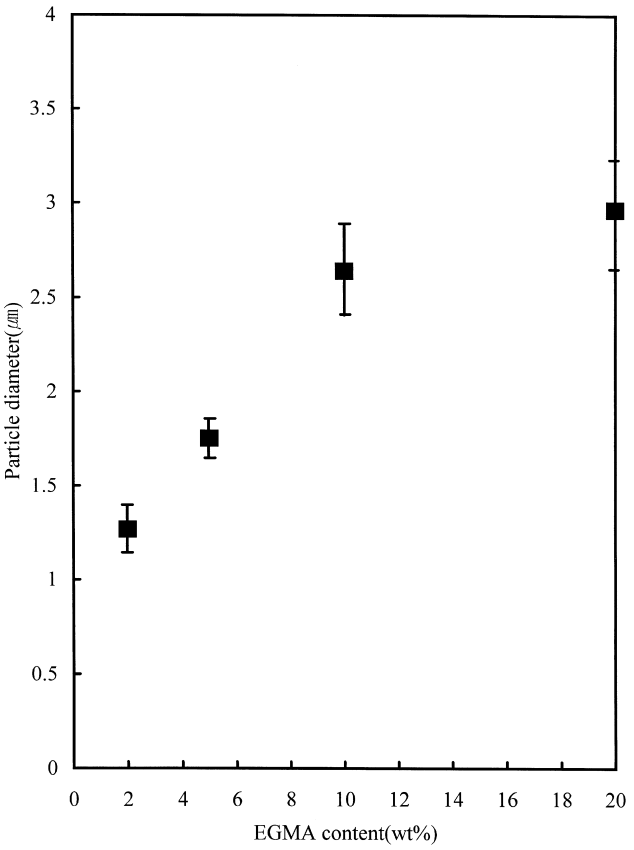

Figure 1 Average EGMA particle size distribution in PPS matrix (bar indicates 95% confidence limit)

According to Van Oene, particles with high elasticity (i.e. higher first normal stress differences, $\sigma_{11} - \sigma_{22}$) tend to increase the interfacial tension in the matrix with relatively low elasticity, and become more stable to the given deformation and result in a poor distribution in the matrix[16]. This probably accounts for the poor distribution of highly elastic EGMA particles in the low elastic PPS matrix. And this coalescence of EGMA particles resulted in the density decrease from the rule of mixtures relationships in the PPS4 and PPS5 blends. Moreover, as the distance between the EGMA particles irregularly decreases, applied stresses can not be evenly distributed within the system and result in the stress concentration in a certain area. Whereas, PPS3 shows an even distribution of EGMA particles and its size distribution is narrow. From these POM observations, 5 wt.% EGMA shows the narrowest distribution of EGMA particles.

Density measurement

Figure 3 shows the densities of PPS/EGMA blends. Density of pure PPS and EGMA was 1.3034 and 0.9782 g cm^{-3}, respectively. Density of PPS3 was slightly higher than the values based on the rule of mixtures relationship which indicates the densification at this particular composition, however, the densities of PPS4 and PPS5 show negative deviation from the rule of mixtures relationship. This

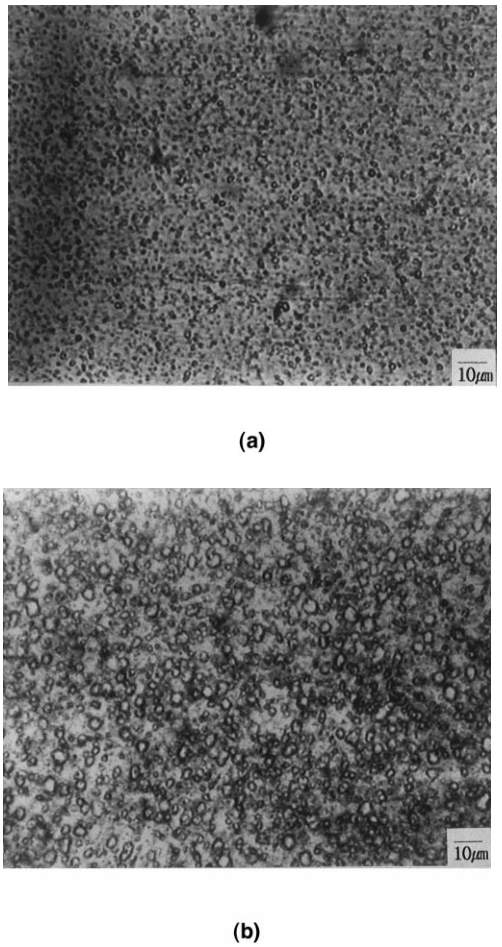

Figure 2 POM micrographs showing EGMA particle size and distribution in PPS matrix (magnification: 400 ×) (a) PPS3, (b) PPS5

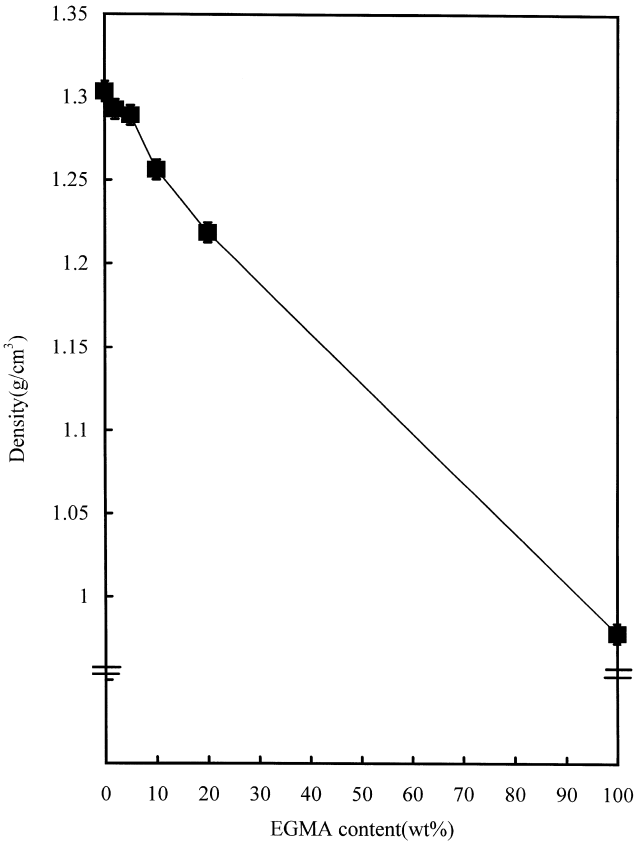

Figure 3 Density of PPS/EGMA blends *versus* EGMA content (bar indicates 95% confidence limit)

phenonmena is probably due to the EGMA particle distribution in a PPS matrix. As can be seen in *Figure 2*, PPS2 and PPS3 have average particle size of less than 2 μm (maximum 2.5 μm, minimum 0.3 μm) and evenly distributed in a matrix. In contrast, PPS4 and PPS5 have average particle size of larger than 2.5 μm (maximum 7.95 μm, minimum 1.2 μm) and uneven distribution which lead to the negative deviation from the rule of mixtures relationship.

Tensile test and morphology

Figure 4a shows the maximum stress of PPS/EGMA blends at different testing temperature conditions. Maximum stress increased up to PPS3 and then decrease above this content when tested at −50°C and 25°C. However, maximum stress was much smaller when tested at 150°C which is a temperature above the T_g of PPS and below T_m of EGMA. *Figure 4b* shows the strain at break of PPS/EGMA blends at the same testing condition. It shows a similar behaviour as in maximum stress tested at −50°C and 25°C, however, at 150°C condition, PPS2 and PPS3 did not break in the thermal chamber, whereas PPS1, PPS4 and PPS5 did break in the thermal chamber. In order to investigate this behaviour, the subsurface and tensile fracture surface of PPS3 and PPS5 was observed using POM and SEM (*Figure 5*). *Figure 5a* shows the subsurface microstructure of PPS3 which was not broken in the thermal chamber. It shows the evenly distributed plastic deformation in the vicinity of EGMA particles parallel to the tensile direction. However, *Figure 5b* shows the subsurface structure of PPS5 and it has uneven plastic deformation and these plastic deformations are localized in the vicinity of the relatively dense and large EGMA particles. These plastic deformations are generally formed 90° to the tensile direction. Due to the localized plastic deformation, fracture can occur in the weak interfacial area between PPS and EGMA and this accounts for the premature failure compared with the PPS2 and PPS3 blends which did not break in the thermal chamber. *Figure 5c* shows the SEM micrograph of tensile fractured surface of PPS5 tested at 150°C, which is the temperature above the T_m of EGMA, thus the EGMA particles melted during the testing, but the space that was occupied by EGMA could be easily observed. However, other SEM micrograph tested below 150°C does not reveal any EGMA particles due to its weak interfacial adhesion, but severe matrix plastic deformation is not observed since PPS has high heat resistance. When EGMA content is less than 10 wt.%, all fracture surfaces show mesa-like morphology[17]. *Figure 5c* shows that the severe plastic deformation occurred where the EGMA particles were closely located, but other areas show a more smooth fracture surface, and this indicates the irregular plastic deformation on the fractured surface.

Figure 4c shows the modulus of elasticity change. At −50°C testing condition, modulus of elasticity does not change much up to PPS4, however, starts to decrease beyond PPS4, and at 25°C testing condition, modulus showed a similar behaviour. At 150°C testing condition, modulus decreased up to PPS3, and then started to increase again at PPS4.

From these results, overall mechanical properties increased up to PPS3 and decreased again above this

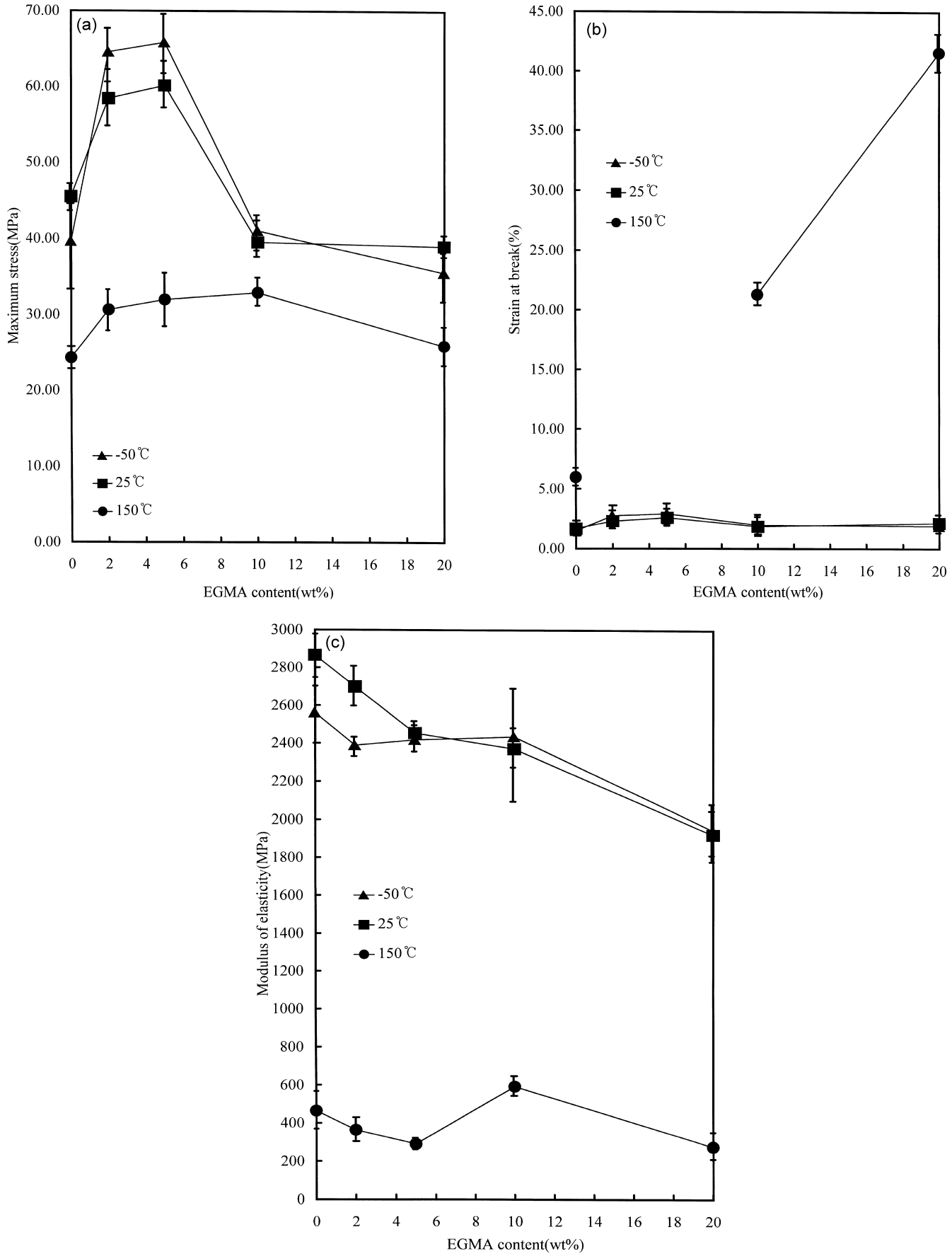

Figure 4 (a) Maximum stress *versus* EGMA content of PPS/EGMA blends at different testing temperatures (bar indicates 95% confidence limit). (b) Strain at break *versus* EGMA content of PPS/EGMA blends at different testing temperatures (bar indicates 95% confidence limit). (c) Modulus of elasticity *versus* EGMA content of PPS/EGMA blends at different testing temperatures (bar indicates 95% confidence limit)

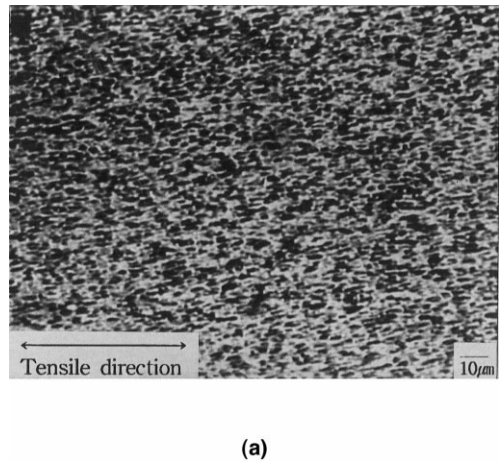

(a)

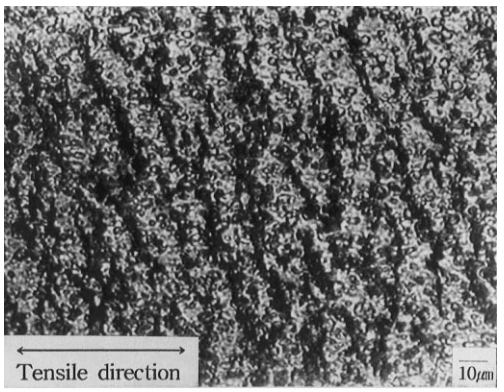

(b)

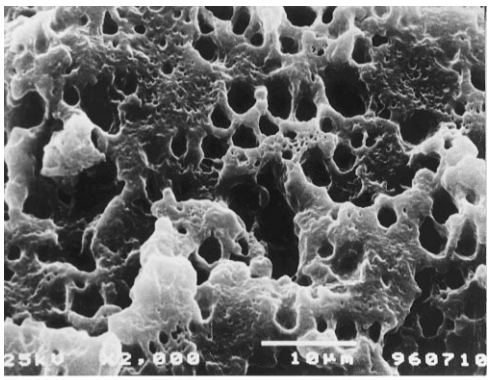

(c)

Figure 5 POM micrographs of tensile tested subsurface microstructure of: (a) PPS3 at 150°C, and (b) PPS5 at 150°C (c) SEM micrograph of tensile fractured surface of PPS5 at 150°C

composition regardless of testing temperatures. Cheung *et al.*[18] explained that the decrease in molecular weight of the dispersed particles was attributed to the mechanical property decrease when PPS occupied 70~80 wt.%. They explained that PPS produces a gas during the injection molding process, and this evaporated gas will damage the polymer chains of EGMA particles and resulted in a decrease of molecular weight. Another possible reasons for the mechanical property decrease in PPS4 and PPS5 is the void formation due to the matrix or dispersed particle contraction. Compounding temperature (315°C–320°C) of PPS/EGMA blends is above its T_m and its mold temperature (80°C) is near the T_m of EGMA. Thus matrix PPS will crystallize first before EGMA particles. This crystallization process will accompany the volume contraction and this contraction will depend on the surface area. As the particles become larger, surface area contraction also become larger, thus it will result in an increase of void space between matrix and dispersed particles. Cheung *et al.*[13] reported the prevention of mechnical property decrease due to this void formation by adding certain amounts of compatibilizer to the blend system.

Impact test and morphology

Figure 6 shows the notched Izod impact strength of PPS/EGMA blends. At all testing temperatures, notched Izod impact strength increased up to PPS3 and started to decrease up to PPS4 and then either increase or decrease depending on the testing temperatures thereafter. *Figure 7* shows the SEM micrographs of impact fractured surfaces of PPS1, PPS3 and PPS5 tested at −50°C. Due to the weak interfacial bonding between PPS and EGMA, dispersed EGMA particles are not found on the fractured surfaces, however, more plastic deformation in PPS3 can be easily found compared to PPS5. This indicates that PPS3 can effectively distribute the impact energy due to the smaller size and even distribution of EGMA particles even though it has weak interfacial adhesion. However, the fracture surface of PPS5 does not show a big difference from pure PPS. These fracture morphology changes are in good agreement with the impact test results, and bigger particle size due to the coalescence and uneven particle size distribution resulted in

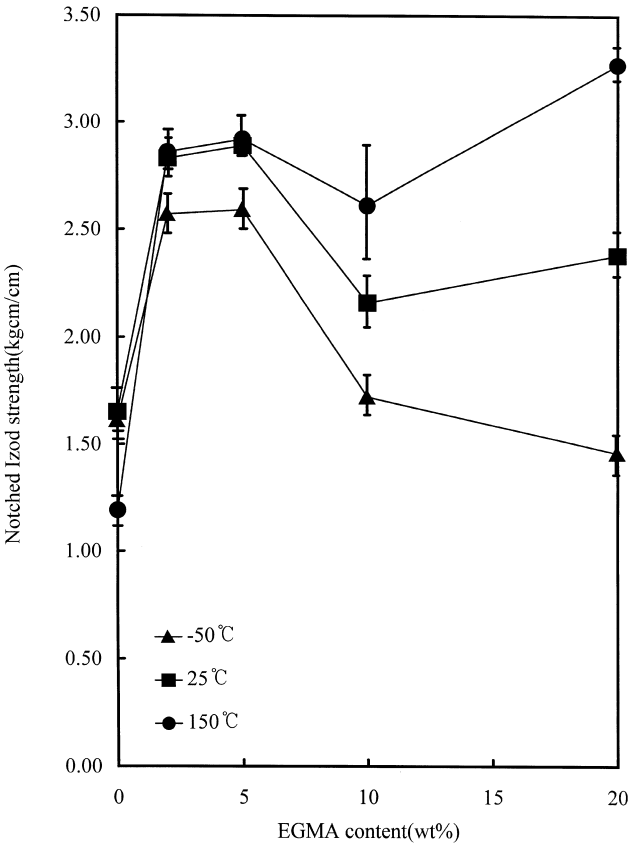

Figure 6 Notched Izod impact strength *versus* EGMA content of PPS/EGMA blends at different testing temperatures (bar indicates 95% confidence limit)

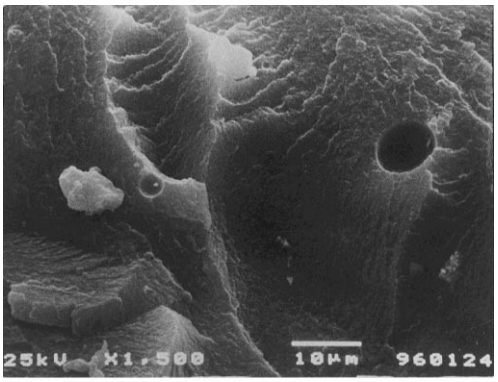

(a)

(b)

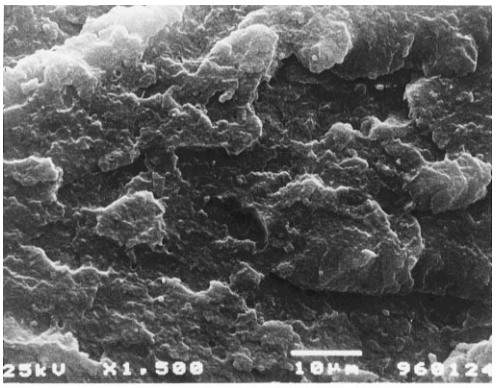

(c)

Figure 7 SEM micrographs of notched Izod impact fracture surface of: (a) pure PPS at −50°C; (b) PPS3 at −50°C; and (c) PPS5 at −50°C

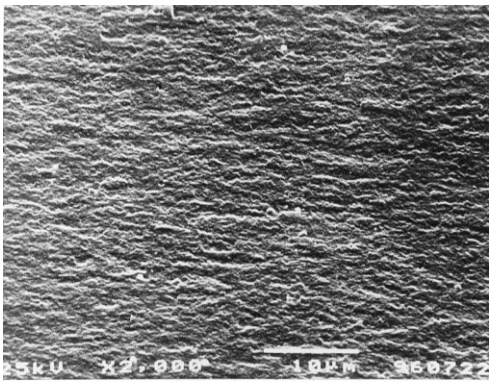

(a)

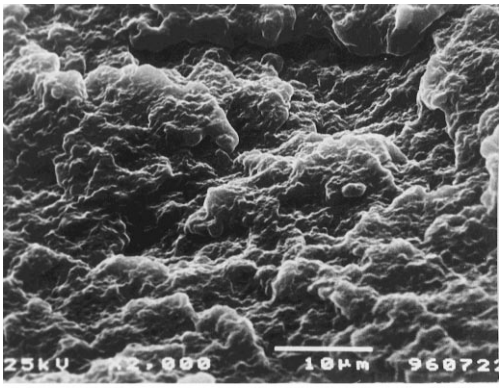

(b)

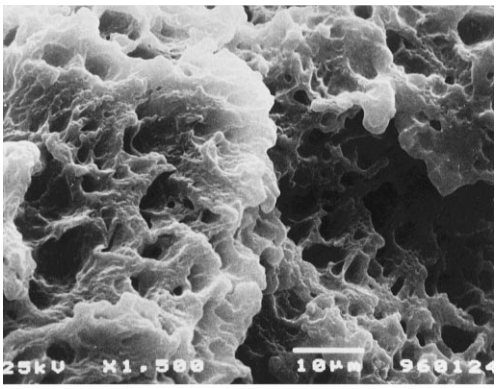

(c)

Figure 8 SEM micrographs of notched Izod impact fracture surface of: (a) pure PPS at 150°C; (b) PPS3 at 150°C; and (c) PPS5 at 150°C

a weak interfacial bonding and impact strength decrease. Generally impact energy can be absorbed by matrix, dispersed particles, and interfacial areas between matrix and dispersed particles. Also, when rubbery particles are blended with brittle matrix, applied energy can be dissipated via craze formation within the matrix. Meanwhile, when brittle particles are dispersed in the tough matrix, energy can be effectively consumed via matrix yielding. Masamoto and Kubo studied the PPS/polyolefin elastomer blends[14], and concluded that the matrix yielding largely account for the absorption of impact energy even though the PPS matrix is brittle. According to their results, when the polyolefin elastomer with a reactive group was blended with untreated PPS, improvement in impact strength was not found. However, when blended with chemically treated PPS, impact strenght increased more then 50 times. They also concluded that depending on the interparticle distance and particle size, brittle-tough transition occurred at a certain interparticle distance and particle size. However, matrix deformation in our study shows typical brittle fracture mode except at 150°C testing condition, and yielding was not observed. Thus in PPS/EGMA blend system, energy dissipation mechanism is due to the energy absorption by crack propagation in the matrix.

Figure 8 shows impact fracture surfaces of PPS1, PPS3 and PPS5 at 150°C testing condition. At −50°C testing

condition, PPS1 shows the irregular sharp fracture patterns like a glass fracture, whereas, *Figure 8a* shows an even PPS plastic deformation in the fracture surface. *Figure 8b* shows an increased plastic deformation and 8*c* shows an even more pronounced plastic deformation. Impact fracture surface of PPS/EGMA blends do not show EGMA particles as in tensile fractured surface, but severe plastic deformation near the space occupied by EGMA particles can be easily observed. However, EGMA particle size of PPS3 is not big enough to show its own area, it is difficult to observe the occupied space as in PPS5. At 150°C testing condition, PPS5 shows a high impact strength due to the wetting of melted EGMA particle to the PPS matrix even though it has poor interfacial bonding. Lange and Radford observed that crazes propagate around the dispersed particles when a craze was initiated in a brittle matrix[19]. Also in our study, when EGMA is more than 10 wt.%, particle size are relatively large (3 mm), thus one can observe craze pinning phenomenon which shows a craze bypass the particles.

CONCLUSIONS

Tensile and impact properties along with resultant fracture morphology of PPS/EGMA blends were investigated at different testing temperatures. Following conclusions can be made.

POM observation of EGMA dispersion within the PPS matrix showed that average EGMA particle size generally increased with EGMA content. However, PPS3 showed the narrowest size distribution of EGMA particles. Density measurement showed that PPS3 had a higher density from the rule of mixtures relationships, whereas PPS4 and PPS5 showed the negative deviation from the rule of mixtures relationships. Maximum stress and strain at break increased up to PPS3 and decreased thereafter. Modulus of elasticity generally decreased with EGMA content and testing temperature. Notched Izod impact strength showed an abrupt increase up to PPS3, and then either increased or decreased thereafter. SEM micrographs of tensile and impact fracture specimens showed a matrix PPS plastic deformation increase with EGMA content and testing temperatures. At all testing temperatures, dispersed EGMA particles could not be found due to either weak interfacial bond or EGMA meltdown. POM observation of fractured and unfractured tensile specimens revealed the plastic deformation parallel to tensile direction in unfractured specimen, whereas, plastic deformation 90° to tensile in fractured specimen.

REFERENCES

1. Jog, J. P. and Nadkarni, V. M., *J. Appl. Polym. Sci.*, 1985, **30**, 997.
2. Seo, K. H., Park, L. S. and Baek, J. B., *Polymer*, 1993, **34**, 2524.
3. Chung, J. S. and Cebe, P., *Polymer*, 1992, **33**, 2312.
4. Chung, J. S. and Cebe, P., *Polymer*, 1992, **33**, 2325.
5. Dai, K. H. and Scobbo, J. J. Jr, *Polym. Bull.*, 1996, **37**, 490.
6. Caramaro, L., Chabert, B. and Chauchard, J., *Polym. Engng Sci.*, 1991, **31**, 1279.
7. Kenny, J. M. and Maffezoli, A., *Polym. Engng Sci.*, 1991, **31**, 607.
8. Park, H. J. and Chun, B. C., *Polym. Bull.*, 1996, **37**, 103.
9. Golovoy, A., Cheung, M. F. and Zinbo, M., *Polym. Comm.*, 1989, **30**, 322.
10. Golovoy, A., Mazioch, K. A., Cheung, M. F. and Berry, V. K., *Polym. Bull.*, 1989, **22**, 175.
11. Zhang, X. and Wang, Y., *Polymer*, 1989, **30**, 1867.
12. Akhtar, S. and White, J. L., *Polym. Engng Sci.*, 1992, **32**, 640.
13. Cheung, M. F., Golovoy, A., Mindroiu, V. E., Plummer, H. K. Jr. and Oene, H. V., *Polymer*, 1993, **34**, 3809.
14. Masamoto, J. and Kubo, K., *Polym. Engng Sci.*, 1996, **36**, 265.
15. Chen, T. H. and Su, A. C., *Polymer*, 1993, **34**, 4826.
16. Oene, H. V., *Colloid Interface Sci.*, 1972, **40**, 440.
17. Cheung, M. F. and Plummer, H. K. Jr., *Polym. Engng Sci.*, 1996, **36**, 15.
18. Cheung, M. F., Golovoy, A. and Oene, H. V., *Polymer*, 1990, **31**, 2307.
19. Lange, F. F. and Radford, K. C., *J. Mater. Sci.*, 1971, **5**, 1197.